

## Peculiar three-dimensional ordering in (In,Ga)As/GaAs(311)B quantum dot superlattices

M. Hanke,<sup>1,a)</sup> M. Schmidbauer,<sup>2</sup> Zh. M. Wang,<sup>3</sup> Yu. I. Mazur,<sup>3</sup> Sh. Seydmohamadi,<sup>3</sup> G. J. Salamo,<sup>3</sup> T. D. Mishima,<sup>4</sup> and M. B. Johnson<sup>4</sup>

<sup>1</sup>Paul-Drude-Institut für Festkörperelektronik, Hausvogteiplatz 5-7, D-10117 Berlin, Germany

<sup>2</sup>Leibniz-Institut für Kristallzüchtung, Max-Born-Straße 2, D-12489 Berlin, Germany

<sup>3</sup>Department of Physics, University of Arkansas, Fayetteville, Arkansas 72701, USA

<sup>4</sup>Homer L. Dodge Department of Physics and Astronomy and Center for Semiconductor Physics in Nanostructures, University of Oklahoma, Norman, Oklahoma 73019, USA

(Received 13 March 2009; accepted 29 April 2009; published online 20 May 2009)

The impact of the GaAs spacer layer thickness on the three-dimensional ordering in (In,Ga)As/GaAs(311)B quantum dot superlattices was investigated by high-resolution x-ray diffraction, cross-sectional transmission electron microscopy, and atomic force microscopy. Dramatic changes in both planar and vertical ordering could be observed. A distinct correlation was found in that the azimuthal angle of inclined vertical inheritance of the dot positions is perpendicular to the planar direction between the dot chains within individual quantum dot layers. These directions are close to [130] or  $[\bar{1}03]$ . © 2009 American Institute of Physics. [DOI: 10.1063/1.3141404]

Lateral and vertical ordering of quantum dots (QDs) are issues of particular interest in semiconductor technology with the ultimate goal of controlling the QD positions. Beyond efforts using lithographic techniques, strain-induced self-formation on the nanometer scale has attracted overwhelming interest during the past decade, e.g., Refs. 1 and 2. The formation of a single nanoscale island can be described in the framework of the Stranski–Krastanow growth mode, where the island formation is mediated by the balance between the surface free energy and the elastic strain energy involved in the growth process. On the other hand, ordering of an ensemble of nanoscale islands is a more complex issue. For growth close to thermodynamic equilibrium, it has been demonstrated that strain-induced kinetic processes play a significant role in the initial pattern formation.<sup>3,4</sup> It has also been shown that anisotropic properties of surfaces may induce alignment of QDs.<sup>5,6</sup> In particular, anisotropic diffusion processes caused by surface reconstruction<sup>7</sup> may result in the formation of extended QD chains.

In the (In,Ga)As/GaAs(100) system, extended and well ordered QD chains oriented along the  $[01\bar{1}]$  direction have been found.<sup>8–10</sup> However, although weak ordering is present for a single layer of (In,Ga)As,<sup>11</sup> the QD chain formation is most pronounced when multiple layers of QDs are stacked to form a three-dimensional (3D) QD lattice. It is, however, interesting to note that lateral and vertical ordering are caused by different mechanisms: the chain formation is mediated by strong anisotropic surface diffusion induced by the  $2 \times 4$  surface reconstruction, while the exact vertical ordering is a result of the elastic properties of the GaAs spacer layer. This behavior was confirmed for (In,Ga)As QD superlattices (SLs) that are grown on high-index GaAs substrates with surface orientations of type  $(n11)B$  ( $n=3,4,5,7,9$ ).<sup>12</sup> Here, inclined vertical inheritance was observed and the derived angles of inheritance strongly depend on the surface orientation. This behavior could be modeled by numerical simulations using linear elasticity theory. On the other hand,

growth on substrates of the type  $(n11)B$  induces an increased surface step density in  $[01\bar{1}]$  direction which strongly influences the atomic diffusion on the surface. This finally leads to QDs arranged in a two-dimensional (2D) rhombic lattice with varying in-plane angle.<sup>6</sup> Vertical and lateral ordering can thus be explained independently and the processes involved surface kinetics for lateral ordering, elastic strain relaxation for vertical arrangement are different.

In this letter we report on the influence of GaAs spacer layer thickness on the 3D ordering in (In,Ga)As/GaAs QD SLs grown on GaAs (311)B substrates. Surprisingly, we found dramatic changes in both vertical and horizontal ordering and, even more importantly, we got strong indications for a remarkable coupling between both. All samples were grown by molecular beam epitaxy. They comprise of 16.5 periods of 10 ML  $\text{In}_{0.4}\text{Ga}_{0.6}\text{As}$ , forming QDs, and subsequent GaAs spacer layers with corresponding thicknesses between 30 and 240 ML. Prior to the SL, a 0.5  $\mu\text{m}$  thick GaAs buffer layer was deposited at 580 °C. This temperature was then decreased to 540 °C for the growth of (In,Ga)As/GaAs SLs. Finally the last  $\text{In}_{0.4}\text{Ga}_{0.6}\text{As}$  QD layer was kept uncovered to enable the investigation of the surface morphology by atomic force microscopy. Corresponding growth rates of  $\text{In}_{0.4}\text{Ga}_{0.6}\text{As}$  and GaAs have been measured using *in situ* reflection high energy electron diffraction, both were kept constant during the experiment at 0.15 and 0.22 ML/s, respectively.

Big changes in the surface morphology can be observed by varying the spacer layer thickness from 30 ML (8 nm) to 240 ML (64 nm) (Fig. 1). The samples with comparatively small spacer layer thicknesses ranging from 30 to 127.5 ML exhibit a 2D dense array of QDs [Figs. 1(a)–1(d)] with improving planar ordering. The highest degree of ordering is achieved at 127.5 ML where a nearly perfect 2D rhombic pattern is observed with the two main directions pointing approximately along [130] and  $[\bar{1}03]$  directions. The 2D pattern abruptly changes when the spacer layer thickness is further increased. Highly ordered QD chains are formed, which are aligned along the [130] direction [Figs. 1(e)–1(g)]. The

<sup>a)</sup>Electronic mail: hanke@pdi-berlin.de.

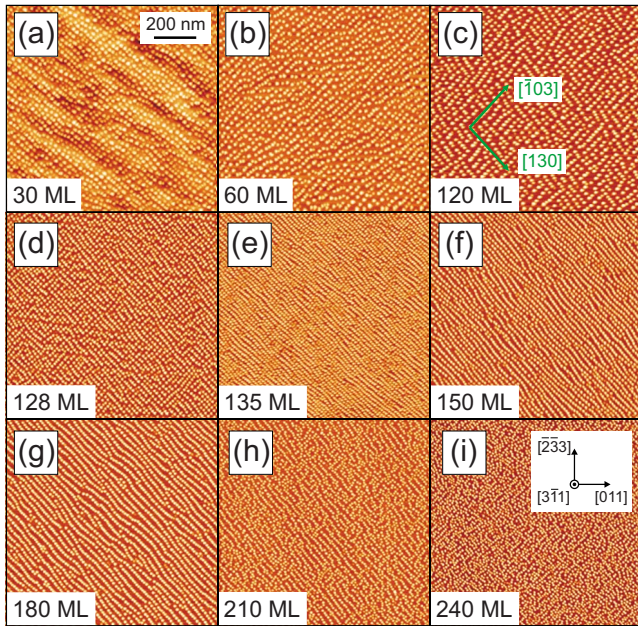


FIG. 1. (Color online) Atomic force micrographs of the topmost surface for various (In,Ga)As/GaAs QD SLs grown on GaAs(311)B. The thickness of the GaAs spacer layers between succeeding QD layers varies between 30 and 240 ML. The green arrows mark the planar [130] and  $[\bar{1}03]$  directions.

highest uniformity is reached when the spacing layer thickness approaches 180 ML. Finally, at very large spacer layer thicknesses, the horizontal ordering is strongly weakened [Figs. 1(h) and 1(i)], which is the case when the vertical correlation between the successive QD layers becomes weaker. The observed large changes in the planar alignment are accompanied by changes in the QD size and density.

In order to determine the 3D arrangement of the QDs, high-resolution x-ray diffraction (HRXRD) has been performed using synchrotron radiation ( $\lambda=1.55 \text{ \AA}$ ) at beamline BW2, HASYLAB (Hamburg, Germany). By using a 2D charged-coupled device detector<sup>13</sup> the intensity distribution of diffuse scattering can be recorded in all three dimensions in the vicinity of the GaAs(311) reciprocal lattice point. Two exemplary 2D sections of the diffuse scattering for 135 ML spacer thickness containing the  $[23\bar{3}]$  and the  $[011]$  direction are displayed in Figs. 2(c) and 2(f), respectively. The diffuse scattering from the QD lattice is concentrated in resonant diffuse scattering (RDS) sheets. The inclination angles of the RDS sheets with respect to the horizontal directions  $[011]$  and  $[23\bar{3}]$  are identical with the corresponding angles of inheritances  $\alpha_{011}$  and  $\alpha_{23\bar{3}}$ , respectively, which are defined in Fig. 3.

In parallel, all samples were probed by cross-sectional transmission electron microscopy (XTEM) within the same crystallographic zones as for HRXRD. The inclination angles can be directly obtained from the XTEM micrographs [see Figs. 2(a) and 2(d) for 135 ML spacer thickness] or, alternatively, from corresponding power spectra [Figs. 2(b) and 2(e)]. The angles derived with XTEM and HRXRD coincide within reasonable agreement (see Table I).

Surprisingly, we observe dramatic changes in both inclination angles  $\alpha_{23\bar{3}}$  and  $\alpha_{011}$  with increasing spacer layer thickness [Table I]. Based on the model discussed in Ref. 12, the finite horizontal size  $w$  of the QDs may reduce the incli-

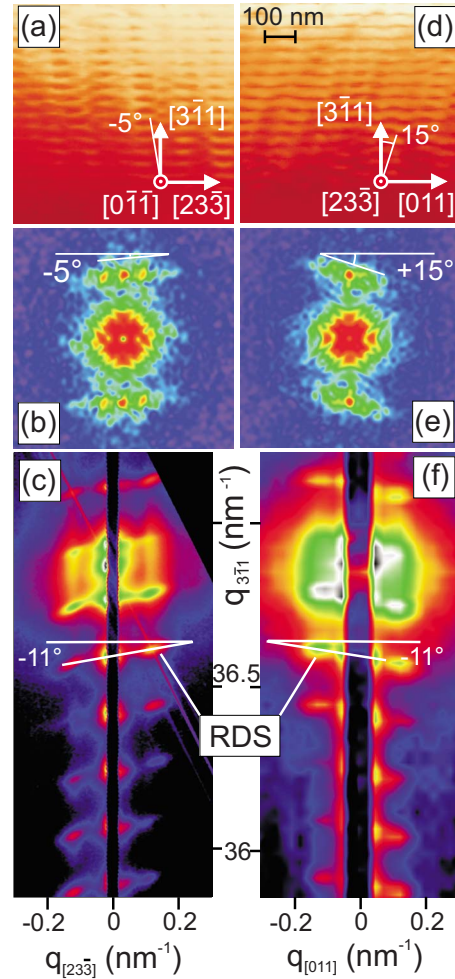


FIG. 2. (Color online) Vertical stack with 135 ML spacer thickness. Bright field XTEM images containing the  $[011]$  (a) and  $[23\bar{3}]$  (d) directions. Corresponding XTEM power spectra (b, e) and HRXRD reciprocal space maps (c, f) were used to deduce the angles of inclined inheritance,  $\alpha_{011}$  and  $\alpha_{23\bar{3}}$ , of the QD stacking in the corresponding projections.

nation angles when the horizontal QD size becomes larger than the spacer layer thickness  $t$ . Otherwise, the inclination angle only depends on the elastic properties of the spacer layer and values of  $\alpha_{23\bar{3}}=10^\circ$  and  $\alpha_{011}=0^\circ$  are expected. Since for all samples  $w < 30 \text{ nm}$  a remarkable reduction in

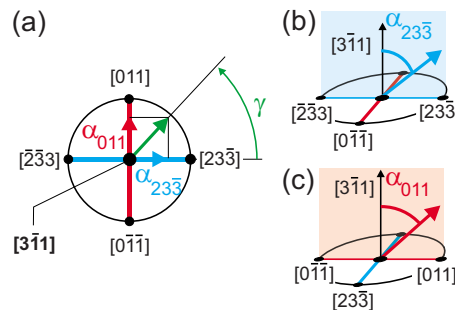


FIG. 3. (Color online) (a) Stereographic projection of the (311)B surface. With respect to the indicated orthogonal directions one can specify the direction of inheritance, which is given by an azimuth  $\gamma$  and a polar angle  $\delta$ , between the direction of inheritance and the growth direction,  $[3\bar{1}1]$ , respectively. However, XTEM as well as HRXRD just probe *projections* of inheritance in particular planes. The two experimental angles (b)  $\alpha_{23\bar{3}}$  and (c)  $\alpha_{011}$  can be used to calculate the azimuthal angle  $\gamma$  and the polar angle  $\delta$  of inclined vertical inheritance.

TABLE I. Projected directions of vertical inheritance as derived from XTEM ( $\alpha_{011}^{\text{XTEM}}, \alpha_{23\bar{3}}^{\text{XTEM}}$ ) compared with x-ray diffraction data ( $\alpha_{011}^{\text{HRXRD}}, \alpha_{23\bar{3}}^{\text{HRXRD}}$ ) as a function of spacer layer thickness  $t$  given in monolayers. The individual differences between the two independent techniques are typically smaller than  $5^\circ$ . From the projected directions the azimuthal ( $\gamma$ ) and polar angle ( $\delta$ ) of inheritance are derived.  $\gamma_{\text{chain}}^\perp$  is the planar direction perpendicular to QD chains.

$t$ (ML)	$\alpha_{011}^{\text{HRXRD}}$	$\alpha_{011}^{\text{XTEM}}$	$\alpha_{23\bar{3}}^{\text{HRXRD}}$	$\alpha_{23\bar{3}}^{\text{XTEM}}$	$\delta$	$\gamma$	$\gamma_{\text{chain}}^\perp$
30	$-23^\circ$	$-20^\circ$	$-28^\circ$	$-30^\circ$	$34^\circ$	$+46^\circ$	$\pm 49^\circ$
60	$+12^\circ$	$+15^\circ$	$-31^\circ$	$-30^\circ$	$32^\circ$	$-19^\circ$	$\pm 54^\circ$
120	$-35^\circ$	$-30^\circ$	$-29^\circ$	$-30^\circ$	$40^\circ$	$+48^\circ$	$\pm 45^\circ$
128	$-29^\circ$	$-30^\circ$	$-20^\circ$	$-25^\circ$	$35^\circ$	$+44^\circ$	$\pm 44^\circ$
135	$+11^\circ$	$+15^\circ$	$-11^\circ$	$-5^\circ$	$15^\circ$	$-44^\circ$	$-45^\circ$
150		$+10^\circ$		$-10^\circ$	$14^\circ$	$-45^\circ$	$-46^\circ$
180	$+12^\circ$	$+10^\circ$	$-11^\circ$	$-10^\circ$	$17^\circ$	$-46^\circ$	$-48^\circ$
210	$+5^\circ$	$+5^\circ$	$-34^\circ$	$-30^\circ$	$32^\circ$	$-7^\circ$	$-45^\circ$
240	$0^\circ$	$0^\circ$	$-11^\circ$	$-10^\circ$	$10^\circ$	$0^\circ$	

the inclination angles can be expected for spacer layer thicknesses below 120 ML only. Therefore, a finite QD size should not be responsible for the observed behavior.

We have already discussed the dramatic changes in QD planar ordering with increasing GaAs spacer layer thickness. A closer inspection of our data reveals a systematic behavior, which suggests a remarkable coupling between planar and vertical ordering. This becomes evident when introducing polar and azimuthal angles of inheritance  $\delta$  and  $\gamma$ , respectively, as defined in Fig. 3. These can be derived from the projected angles  $\alpha_{011}$  and  $\alpha_{23\bar{3}}$  by using the expressions  $\tan \gamma = \tan \alpha_{23\bar{3}} / \tan \alpha_{011}$  and  $\tan \delta = \sqrt{\tan^2 \alpha_{23\bar{3}} + \tan^2 \alpha_{011}}$ . In Fig. 4(a), the polar angle  $\delta$  of inclined inheritance is plotted as a function of the spacer layer thickness  $t$ . It abruptly changes from values around  $\delta = 35^\circ$  at  $t$  smaller than about 130 ML (2D rhombic planar ordering) to values around  $\delta = 15^\circ$  at  $t$  larger than 130 ML (one-chain formation). Even more striking is the behavior of the azimuthal angle  $\gamma$ , which is always close to  $\pm 45^\circ$ . The azimuthal direction of inclined inheritance is thus parallel to either  $[130]$  or  $[\bar{1}03]$ . On the other hand these directions characterize the planar ordering. This is quantitatively illustrated in Fig. 4(b), where the azimuthal angle  $\gamma$  of inclined vertical inheritance and the azimuthal angle  $\gamma_{\text{chain}}^\perp$  are plotted as a function of the spacer layer thickness. The 3D ordering thus undergoes a “phase transition” at about 130 ML GaAs spacer layer thickness.

In conclusion, we reported on a systematic study on the influence of the GaAs spacer layer thickness on the 3D arrangement in (In,Ga)As/GaAs QD SLs. We found dramatic changes in both planar and vertical ordering. However, these changes seem to follow a common rule in that the azimuthal angle of inheritance and the direction perpendicular to the QD chains point into the same direction, which is very close either to  $[130]$  or to  $[\bar{1}03]$ . A detailed understanding of the observed peculiar 3D ordering is still missing. Kinetic Monte Carlo simulations of 3D QD lattices, however, predict a sharp transition between correlated and anticorrelated growth as a function of the spacer layer thickness quite similar to the behavior displayed in Fig. 4.

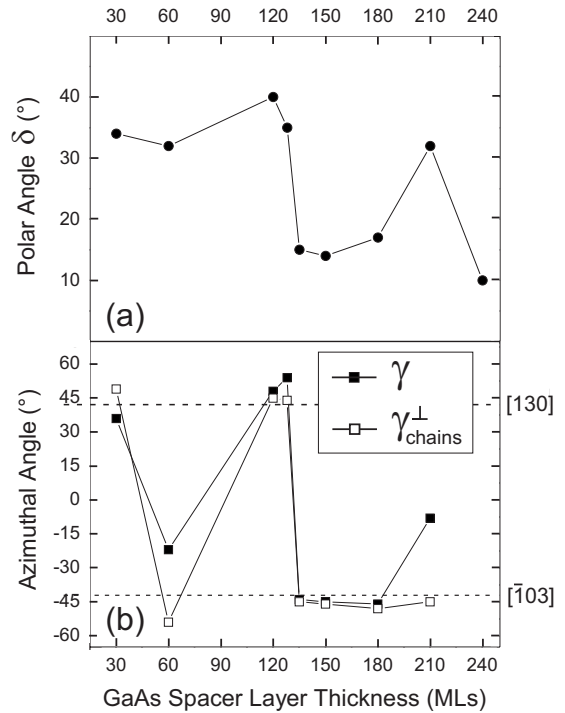


FIG. 4. (a) Polar ( $\delta$ ) and (b) azimuthal angle ( $\gamma$ ) of inclined vertical inheritance as a function of GaAs spacer layer thickness. Also plotted is the direction perpendicular to the observed QD chain direction  $\gamma_{\text{chain}}^\perp$ , which is in good agreement with  $\gamma$ . The dashed lines mark the planar  $[130]$  and  $[\bar{1}03]$  directions.

This work was financially supported by the Federal State of Sachsen-Anhalt, Germany, within the research network *Nanostructured Materials*, project NW3. We thank the Hamburg Synchrotron Radiation Laboratory HASYLAB, for providing beamtime. Assistance with the experiment by P.Schäfer (Humboldt-University, Berlin) and D.Grigoriev (University of Karlsruhe) is highly appreciated.

- <sup>1</sup>V. A. Shchukin, N. N. Ledentsov, and D. Bimberg, *Epitaxy of Nanostructures* (Springer, New York, 2004).
- <sup>2</sup>O. G. Schmidt, *Lateral Alignment of Epitaxial Quantum Dots* (Springer, Berlin, 2007).
- <sup>3</sup>M. Meixner, E. Schöll, M. Schmidbauer, H. Raidt, and R. Köhler, *Phys. Rev. B* **64**, 245307 (2001).
- <sup>4</sup>M. Hanke, H. Raidt, R. Köhler, and H. Wawra, *Appl. Phys. Lett.* **83**, 4927 (2003).
- <sup>5</sup>D. Bimberg, M. Grundmann, and N. N. Ledentsov, *Quantum Dot Heterostructures* (Wiley, New York, 1999).
- <sup>6</sup>Z. M. Wang, C. Rodriguez, S. Seydmohmadi, Yu. I. Mazur, Y. Z. Xie, and G. J. Salamo, *Appl. Phys. Lett.* **94**, 083107 (2009).
- <sup>7</sup>C. Teichert, *Phys. Rep.* **365**, 335 (2002).
- <sup>8</sup>Z. M. Wang, K. Holmes, Yu. I. Mazur, and G. J. Salamo, *Appl. Phys. Lett.* **84**, 1931 (2004).
- <sup>9</sup>F. Poser, A. Bhattacharya, S. Weeke, and W. Richter, *J. Cryst. Growth* **248**, 317 (2003).
- <sup>10</sup>M. Hanke, Z. M. Wang, Yu. I. Mazur, J. H. Lee, G. J. Salamo, and M. Schmidbauer, *Appl. Phys. Lett.* **92**, 033111 (2008).
- <sup>11</sup>M. Schmidbauer, Z. M. Wang, Yu. I. Mazur, P. M. Lytvyn, G. J. Salamo, D. Grigoriev, P. Schäfer, R. Köhler, and M. Hanke, *Appl. Phys. Lett.* **91**, 093110 (2007).
- <sup>12</sup>M. Schmidbauer, S. Seydmohmadi, D. Grigoriev, Z. M. Wang, Yu. I. Mazur, P. Schäfer, M. Hanke, R. Köhler, and G. J. Salamo, *Phys. Rev. Lett.* **96**, 066108 (2006).
- <sup>13</sup>M. Schmidbauer, P. Schäfer, S. Besedin, D. Grigoriev, R. Köhler, and M. Hanke, *J. Synchrotron Radiat.* **15**, 549 (2008).